BNL-101523-2014-TECH
AD/AP 33;BNL-101523-2013-IR

The Thick Ellipse Effect Due to Linear Coupling, and Projections of the Invariant 4-Ellipsoid onto the (x,x), (y, y) and the (x,y)-Planes

V. Garczynski

December 1991

Collider Accelerator Department
Brookhaven National Laboratory

U.S. Department of Energy
USDOE Office of Science (SC)

DISCLAIMER

AD/AP-33

Accelerator Development Department
Accelerator Physics Division
BROOKHAVEN NATIONAL LABORATORY
Associated Universities, Inc.
Upton, NY 11973

Accelerator Physics Technical Note No. 33

The Thick Ellipse Effect Due to Linear Coupling, and Projections of the Invariant 4-Ellipsoid onto the (x, x'), (y, y') and the (x, y)-Planes

V. Garczynski

December 1991

THE THICK ELLIPSE EFFECT DUE TO LINEAR COUPLING, AND PROJECTIONS OF THE INVARIANT 4-ELLIPSOID ONTO THE (x, x'), (y, y') AND THE (x, y)-PLANES

V. Garczynski

Accelerator Development Department
Brookhaven National Laboratory

December 1991

Contents

THE THICK ELLIPSE EFFECT DUE TO LINEAR COUPLING, AND PROJECTIONS OF THE INVARIANT 4-ELLIPSOID ONTO THE (x, x'), (y, y') AND THE (x, y)-PLANES

V. Garczynski
Accelerator Development Department
Brookhaven National Laboratory
December 1991

1. Introduction

Coupling between the transverse x and y degrees of freedom causes phase plots (x, x') or (y, y') that are thick ellipses, (the Thick Ellipse Effect). This effect is produced in computer simulations of the x-y coupling existing in RHIC; a smear of the familiar Courant-Snyder ellipses (or, rather, circles in suitably normalized coordinates) is produced in, both, (x, x'), and (y, y')-planes.[1,2] The smear presented in Fig. 1 corresponds to plotting of the (x, x'), and the (y, y') components of finite, discrete set of points

$$T(z_0),\ T(T(z_0)),\ \ldots,\underbrace{T(\ldots T(T}_{1000}(z_0))\ldots). \tag{1.1}$$

This effect is somewhat dependent on the choice of the initial 4-vector z_0, and on the nonlinear couplings included in the single-turn map T. It is not excluded that more of the phase-space would be covered, including central parts, if different initial vectors would be employed.

In the paper we examine the linearly coupled motion produced by thin skew-quadrupoles distributed around a ring, and determine their contribution to the Thick Ellipse Effect.

We reveal the main driving terms responsible for the spread of the invariant curves. We also show that the spread is removed, at the point where the tune splitting correction is made.

In order to be able to accommodate any trajectory, corresponding to any choice of the initial conditions and number of turns, we are looking for the total areas in the physical subspaces, i.e. (x, x'), (y, y') and (x, y) subspaces, which are available for the motion. They are given by projections of the invariant 4-Ellipsoid onto the (x, x'), (y, y') and the (x, y)-planes. Since the invariant 4-Ellipsoid replaces familiar Courant-Snyder curves, when the linear coupling is present, we study this rather novel object, in some detail, first.

As usual, $\partial\mathcal{E}_4$ denotes a two-dimensional surface of the solid four-dimensional ellipsoid $\mathcal{E}_4$. Similar for the lower-dimensionality geometric objects appearing in the sequel.

2. The Equations of Motion

We consider the betatron motion under presence of the linear coupling produced by skew-quadrupole fields. The Hamiltonian of the system is quadratic

$$H = \frac{1}{2}p_x^2 + \frac{1}{2}p_y^2 + \frac{1}{2}\left(\rho^{-2} - k\right)x^2 + \frac{1}{2}ky^2 - Nxy. \tag{2.1}$$

Hamilton's equations of motion are linear, with periodic coefficients

$$\begin{aligned} x' &= p_x, \\ p_x' &= \left(k - \rho^{-2}\right)x + Ny, \\ y' &= p_y', \\ p_y' &= -ky + Nx. \end{aligned} \tag{2.2}$$

They can be cast in the form of the second-order differential equations

$$\begin{aligned} x'' + \left(\rho^{-2} - k\right)x &= Ny, \\ y'' + ky &= Nx. \end{aligned} \tag{2.3}$$

Any solution can be written in the form

$$z(s) = T(s, s_0)\, z(s_0), \tag{2.4}$$

where

$$z = \begin{pmatrix} x \\ x' \\ y \\ y' \end{pmatrix}, \tag{2.5}$$

and T is a real 4×4 transfer matrix satisfying the symplecticity condition

$$\tilde{T}ST = S, \tag{2.6}$$

where

$$S = \begin{pmatrix} \sigma & \mathbf{0} \\ \mathbf{0} & \sigma \end{pmatrix}, \tag{2.7}$$

and

$$\sigma = \begin{pmatrix} 0 & 1 \\ -1 & 0 \end{pmatrix}. \tag{2.8}$$

It is well known,[2] that there exists a real 4×4 symplectic matrix-R, such that when passing to new variables $w = R^{-1}z$

$$w = \begin{pmatrix} u \\ u' \\ v \\ v' \end{pmatrix} = \begin{pmatrix} U \\ V \end{pmatrix}, \tag{2.9}$$

the motions decouple, i.e.,

$$w(s) = U(s, s_0)\, w(s_0), \tag{2.10}$$

where

$$U = R^{-1}TR = \begin{pmatrix} A & \mathbf{0} \\ \mathbf{0} & B \end{pmatrix}. \tag{2.11}$$

The submatrices A, B are real 2×2 symplectic matrices describing the uncoupled betatron motions, which can be described by the Courant-Snyder parameters. For the single turn transfer matrix T, we have for the A, B submatrices

$$A = \mathbf{1} \cos \mu_1 + \mathbf{J_1} \sin \mu_1, \tag{2.12}$$

$$B = \mathbf{1} \cos \mu_2 + \mathbf{J_2} \sin \mu_2, \tag{2.13}$$

where the matrices $\mathbf{J_k}$ are C-periodic (C-circumference) and symplectic

$$\mathbf{J_k} = \begin{pmatrix} \alpha_k & \beta_k \\ -\gamma_k & -\alpha_k \end{pmatrix}, \tag{2.14}$$

$$|\mathbf{J_k}| = \gamma_k \beta_k - \alpha_k^2 = 1, \quad k = 1, 2. \tag{2.15}$$

The α_k, β_k, γ_k, and μ_k are called the new parameters, and they replace the familiar Courant-Snyder parameters pertinent to the uncoupled x-y motion.

3. Digression on Invariants

It follows from the symplecticity conditions (2.6) that, for any natural number k, the combinations

$$\tilde{z}ST^k z; \quad k = 1, 2, \ldots, \tag{3.1}$$

are independent of the s-variable; they are invariants. They can also be expressed via the w-variables as follows

$$\begin{aligned}
&\tilde{z}ST^k z = \tilde{w}SU^k w = \\
&= \tilde{U}\sigma \mathbf{J}_1 U \sin(k\mu_1) + \tilde{V}\sigma \mathbf{J}_2 V \sin(k\mu_2) = \\
&= -\frac{1}{\beta_1}\left[u^2 + (\alpha_1 u + \beta_1 u')^2\right]\sin(k\mu_1) - \\
&- \frac{1}{\beta_2}\left[v^2 + (\alpha_2 v + \beta_2 v')^2\right]\sin(k\mu_2) = \\
&= -\epsilon_1 \sin(k\mu_1) - \epsilon_2 \sin(k\mu_2), \quad k = 1, 2.
\end{aligned} \tag{3.2}$$

One sees, that there are only two independent invariants

$$\begin{aligned}
&W_1 = \tilde{U}\sigma \mathbf{J}_1 U = \\
&= \tilde{w}S\begin{pmatrix} \mathbf{J}_1 & \mathbf{0} \\ \mathbf{0} & \mathbf{0} \end{pmatrix} w = \\
&= \tilde{z}SR\begin{pmatrix} A & \mathbf{0} \\ \mathbf{0} & \mathbf{0} \end{pmatrix} R^{-1} z (\sin\mu_1)^{-1} = -\epsilon_1 < 0,
\end{aligned} \tag{3.3}$$

and

$$\begin{aligned}
&W_2 = \tilde{V}\sigma \mathbf{J}_2 V = \\
&= \tilde{w}S\begin{pmatrix} \mathbf{0} & \mathbf{0} \\ \mathbf{0} & \mathbf{J}_2 \end{pmatrix} w = \\
&= \tilde{z}SR\begin{pmatrix} \mathbf{0} & \mathbf{0} \\ \mathbf{0} & B \end{pmatrix} R^{-1} (\sin\mu_2)^{-1} = -\epsilon_2 < 0.
\end{aligned} \tag{3.4}$$

When the new tunes coincide

$$\mu_1 = \mu_2 = \mu, \tag{3.5}$$

i.e., when the tune splitting is corrected, the invariants coincide, up to a factor

$$\tilde{z}ST^k z = \tilde{z}STz \cdot \sin(k\mu)(\sin\mu)^{-1}. \tag{3.6}$$

This comes about since all the invariants are proportional to a sum $W_1 + W_2$, in this case. Thus, it is sufficient to study only the simplest, linear in T invariant

$$\tilde{z}STz = \tilde{w}SUw = -\epsilon \sin\mu_1 - \epsilon_2 \sin\mu_2 = \lambda. \tag{3.7}$$

Since in RHIC, the tunes $\mu_x \simeq \mu_1 \simeq \mu_y \simeq \mu_2$ are such that $\sin \mu_x$ and $\sin \mu_y$ are negative, we restrict our attention to the case when the parameter λ is a positive constant,

$$\lambda > 0. \tag{3.8}$$

This defines the basic object of our further study - the invariant 4-Ellipsoid, $\partial \mathcal{E}_4$, in the phase-space, given by Eq. (3.7), and the condition (3.8).

One knows that if n-ellipsoid equation is cast into the form

$$\tilde{z} \sigma^{-1} z = 1, \tag{3.9}$$

where σ is a positive-definite symmetric matrix, the volume it includes is given by the formula

$$V_n = \left[\Gamma\left(n/2+1\right)\right]^{-1} \left(\det \sigma\right)^{1/2}. \tag{3.10}$$

In our case the matrix σ^{-1} is, after a symmetrization, given by the expression

$$\sigma^{-1} = (2\lambda)^{-1} S\left(T - T^{-1}\right). \tag{3.11}$$

In general, it possesses an inverse, and leads to a finite (four-dimensional) volume. This is not true for the invariants W_1, W_2 since the corresponding kernels σ_1^{-1}, σ_2^{-1} are degenerate, as it is seen from the formulae (3.3) and (3.4). Two of the eigenvalues of each kernel are zero, and any growth in the corresponding eigen-directions is not contained. Thus neither one of them individually describes a bounded region in the four-dimensional phase-space.

4. The Machine 4-Ellipsoid

The equation (3.10) of the 4-Ellipsoid $\partial\mathcal{E}_4$ can be written in the components

$$\tilde{z}STz = \sum_{k,\ell=1}^{4} F_{k\ell} z_k z_\ell = \lambda. \tag{4.1}$$

Here, T stands for a single turn transfer matrix calculated at the observation point $s = 0$.

It is by now customary to work with, so-called, normalized coordinates, $\overset{\circ}{z}$, defined by the relation, (the circular representation),

$$\overset{\circ}{z} = \mathcal{B}z, \tag{4.2}$$

where the 4×4 matrix $\mathcal{B}$ is of the form

$$\mathcal{B} = \begin{pmatrix} \mathcal{B}_x & \mathbf{0} \\ \mathbf{0} & \mathcal{B}_y \end{pmatrix}, \tag{4.3}$$

and

$$\mathcal{B}_x = \begin{pmatrix} \mathcal{B}_x^{1/2} & 0 \\ \alpha_x \beta_x^{-1/2} & \beta_x^{1/2} \end{pmatrix}, \quad \mathcal{B}_x^{-1} = \begin{pmatrix} \beta_x^{1/2} & 0 \\ -\alpha_x \beta_x^{-1/2} & \beta_x^{-1/2} \end{pmatrix}, \tag{4.4}$$

and similar for $\mathcal{B}_y$, $\mathcal{B}_y^{-1}$. The α_x and β_x functions are those of a perfect machine - without the linear coupling. We assume, additionally, that at the observation point, the α_x and α_y vanish

$$\alpha_x(0) = \alpha_y(0) = 0. \tag{4.5}$$

Hence, we have the usual relations between the coordinates, at the point $s = 0$,

$$\begin{aligned} x &= \beta_x^{1/2}\, \overset{\circ}{x}, \\ x' &= \beta_x^{-1/2}\, \overset{\circ}{x}', \\ y &= \beta_y^{1/2}\, \overset{\circ}{y}, \\ y' &= \beta_y^{-1/2}\, \overset{\circ}{y}'. \end{aligned} \tag{4.6}$$

Taking into account the fact that

$$\tilde{\mathcal{B}}^{-1} S \tilde{\mathcal{B}} = S, \tag{4.7}$$

one gets

$$\tilde{z}STz = \tilde{z}Fz = \overset{\tilde{\circ}}{z} \overset{\circ}{F} \overset{\circ}{z} = \overset{\tilde{\circ}}{z}\, S\, \overset{\circ}{T} \overset{\circ}{z}, \tag{4.8}$$

where

$$\overset{\circ}{T} = \mathcal{B}T\mathcal{B}^{-1} = \begin{pmatrix} \overset{\circ}{M} & \overset{\circ}{n} \\ \overset{\circ}{m} & \overset{\circ}{N} \end{pmatrix}, \tag{4.9}$$

is the single turn transfer matrix in the circular representation. Hence, the coefficients $\overset{\circ}{F}_{k\ell}$ are

$$\overset{\circ}{F}_{k\ell} = \left(S\,\overset{\circ}{T}\right)_{k\ell} = \begin{pmatrix} \overset{\circ}{M}_{21} & \overset{\circ}{M}_{22} & \overset{\circ}{n}_{21} & \overset{\circ}{n}_{22} \\ -\overset{\circ}{M}_{11} & -\overset{\circ}{M}_{12} & -\overset{\circ}{n}_{11} & -\overset{\circ}{n}_{12} \\ \overset{\circ}{m}_{21} & \overset{\circ}{m}_{22} & \overset{\circ}{N}_{21} & \overset{\circ}{N}_{22} \\ -\overset{\circ}{m}_{11} & -\overset{\circ}{m}_{12} & -\overset{\circ}{N}_{11} & -\overset{\circ}{N}_{12} \end{pmatrix}. \tag{4.10}$$

Notice, they are not symmetric in their indices k, ℓ. The coefficients $F_{k\ell}$ can be found from the relation

$$F = \tilde{\mathcal{B}}\,\overset{\circ}{F}\,\mathcal{B}. \tag{4.11}$$

It appears useful to consider symmetrized coefficients given by the expansion

$$\begin{aligned} &\overset{\circ}{\tilde{z}}\,S\,\overset{\circ}{T}\overset{\circ}{z} = \\ &= F_{xx}x^2 + 2F_{xx'}xx' + 2F_{xy}xy + 2F_{xy'}xy' + F_{x'x'}x'^2 + \\ &+ 2F_{x'y}x'y + 2F_{x'y'}x'y' + F_{yy}y^2 + 2F_{yy'}yy' + F_{y'y'}y'^2 = \lambda. \end{aligned} \tag{4.12}$$

We dropped the little circles above since we will work, exclusively, with the circular representation. The new coefficients are related to the previous, and to the transfer matrix elements, as follows

$$\begin{aligned} F_{xx} &= F_{11} = \overset{\circ}{M}_{21}, \\ 2F_{xx'} &= F_{12} + F_{21} = \overset{\circ}{M}_{22} - \overset{\circ}{M}_{11}, \\ 2F_{xy} &= F_{13} + F_{31} = \overset{\circ}{n}_{21} + \overset{\circ}{m}_{21}, \\ 2F_{xy'} &= F_{14} + F_{41} = \overset{\circ}{n}_{22} - \overset{\circ}{m}_{11}, \\ F_{x'x'} &= F_{22} = -\overset{\circ}{M}_{12}, \\ 2F_{x'y} &= F_{23} + F_{32} = \overset{\circ}{m}_{22} - \overset{\circ}{n}_{11}, \\ 2F_{x'y'} &= F_{24} + F_{42} = -\overset{\circ}{n}_{12} - \overset{\circ}{m}_{12}, \\ F_{yy} &= F_{33} = \overset{\circ}{N}_{21}, \\ 2F_{yy'} &= F_{34} + F_{43} = \overset{\circ}{N}_{22} - \overset{\circ}{N}_{11}, \\ F_{y'y'} &= F_{44} = -\overset{\circ}{N}_{12}\,. \end{aligned} \tag{4.13}$$

The positive-definiteness of the quadratic form (4.12) implies the following inequalities

$$F_{xx} > 0, \tag{4.14}$$

$$\begin{vmatrix} F_{xx} & F_{xx'} \\ F_{x'x} & F_{x'x'} \end{vmatrix} = F_{xx}F_{x'x'} - F_{xx'}^2 > 0, \tag{4.15}$$

and similar for the third, and for the fourth-order principal minors. Another three more sets of the inequalities can be obtained from the previous one upon the cyclic permutation of the variables x, x', y, y'.

It is clear, that the projection of the $\partial\mathcal{E}_4$ onto, let say, (x, x')-plane will contain, together with a boundary curve, all the internal points, as well. In particular, it will include the origin $x = 0$, $x' = 0$, since, for this point, one gets from Eq. (4.12) the condition

$$F_{yy}y^2 + 2F_{yy'}yy' + F_{y'y'}y'^2 = \lambda. \tag{4.16}$$

The whole ellipse, in the (y, y')-plane, corresponds to the origin in the (x, x')-plane, and vice-versa.

5. Expression of the 4-Ellipsoid's Coefficients Through the Driving Terms

Using the relation (4.13), and our knowledge of the single-turn transfer matrix derived from the thin lens, discrete model[3-6] we can express the coefficients F_{xx}, etc., through the driving terms. It is assumed here that the N thin skew-quadrupoles of strengths q_k, and location s_k are distributed around a ring

$$q_k = (\beta_x \beta_y)^{1/2} \rho^{-1} \ell_k a_1 \Big|_{s_k}, k = 1, \ldots, N. \tag{5.1}$$

The single-turn transfer matrix can be written as a polynomial in the q's

$$T = \sum_{k=0}^{N} T^{(k)}, \tag{5.2}$$

where $T^{(k)}$ can be expressed via the k-th order in the q's, driving terms. We list the 4-Ellipsoid's coefficients, up to the second order in the q's.

$$F_{xx} = -\sin\mu_x + d_{sc}^{(2)} \sin\mu_x + d_{cc}^{(2)} \cos\mu_x + \ldots, \tag{5.3}$$

$$2F_{xx'} = d_{ss}^{(2)} \sin\mu_x + d_{sc}^{(2)} \cos\mu_x + d_{cs}^{(2)} \cos\mu_x - d_{cc}^{(2)} \sin\mu_x + \ldots, \tag{5.4}$$

$$2F_{xy} = d_{sc}^{(1)} \sin\mu_x + d_{cs}^{(1)} \sin\mu_y + d_{cc}^{(1)} (\cos\mu_x + \cos\mu_y) + \ldots = 2\check{F}_{xy}, \tag{5.5}$$

$$2F_{xy'} = d_{ss}^{(1)} \sin\mu_y + d_{cs}^{(1)} (\cos\mu_x + \cos\mu_y) - d_{cc}^{(1)} \sin\mu_y + \ldots, \tag{5.6}$$

$$F_{x'x'} = -\sin\mu_x + d_{ss}^{(2)} \cos\mu_x - d_{cs}^{(2)} \sin\mu_x + \ldots, \tag{5.7}$$

$$2F_{x'y} = 2\check{F}_{xy'}, \tag{5.8}$$

$$2F_{x'y'} = d_{ss}^{(1)} (\cos\mu_x + \cos\mu_y) - d_{sc}^{(1)} \sin\mu_y - d_{cs}^{(1)} \sin\mu_x + \ldots = 2\check{F}_{x'y'}, \tag{5.9}$$

$$F_{yy} = \check{F}_{xx}, \tag{5.10}$$

$$2F_{yy'} = 2\check{F}_{xx'}, \tag{5.11}$$

$$F_{y'y'} = \check{F}_{x'x'}. \tag{5.12}$$

Here the driving terms of the first order $d^{(1)}$ and of the second order $d^{(2)}$ are defined as follows

$$\begin{pmatrix} d_{ss}^{(1)} \\ d_{sc}^{(1)} \\ d_{cs}^{(1)} \\ d_{cc}^{(1)} \end{pmatrix} = \sum_{r=1}^{N} q_r \begin{pmatrix} \sin\mu_x^r & \sin\mu_y^r \\ \sin\mu_x^r & \cos\mu_y^r \\ \cos\mu_x^r & \sin\mu_y^r \\ \cos\mu_x^r & \cos\mu_y^r \end{pmatrix}, \tag{5.13}$$

and

$$\begin{pmatrix} d^{(2)}_{ss} \\ d^{(2)}_{sc} \\ d^{(2)}_{cs} \\ d^{(2)}_{cc} \end{pmatrix} = \sum_{1\le r<s\le N} q_r q_s \sin\left(\mu^s_x - \mu^r_y\right) \begin{pmatrix} \sin\mu^s_x & \sin\mu^r_x \\ \sin\mu^s_x & \cos\mu^r_x \\ \cos\mu^s_x & \sin\mu^r_x \\ \cos\mu^s_x & \cos\mu^r_x \end{pmatrix}, \tag{5.14}$$

and μ^r_x, μ^r_y are phase advances

$$\mu^r_x = \int_0^{s_r} \frac{ds}{\beta_x}, \quad \mu^r_y = \int_0^{s_r} \frac{ds}{\beta_y}. \tag{5.15}$$

Additional sets of driving terms, denoted as $\check{d}^{(1)}_{ss}$, $\check{d}^{(2)}_{ss}$, etc. are obtained from the above equations by simply exchanging x and y, x' and y' inside of it. That is by the operation

$$z = \begin{pmatrix} x \\ x' \\ y \\ y' \end{pmatrix} \longrightarrow \begin{pmatrix} y \\ y' \\ x \\ x' \end{pmatrix} = \check{z}. \tag{5.16}$$

In our case this yields simply

$$\check{d}^{(k)}(x,y) = d^{(k)}(y,x), \quad k = 1,2, \tag{5.17}$$

and similar for the conjugate coefficients $\check{F}$.

6. Symmetries of the 4-Ellipsoid

Due to the relations (5.3) - (5.12) between the coefficients F and their conjugates $\check{F}$, one may rewrite the equation (4.12) for the 4-Ellipsoid in the form

$$\begin{aligned} &F_{xx}x^2 + 2F_{xx'}xx' + F_{xy}xy + 2F_{xy'}xy' + F_{x'x'}x'^2 + F_{x'y'}x'y' + \\ &+ \left(F_{xx}x^2 + 2F_{xx'}xx' + F_{xy}xy + 2F_{xy'}xy' + F_{x'x'}x'^2 + F_{x'y'}x'y'\right)^{\mathrm{v}} = \lambda. \end{aligned} \tag{6.1}$$

One notices immediately that this equation stays unchanged under the two different transformations:

$$1^o \quad z \to -z, \tag{6.2}$$

$$2^o \quad z \to \check{z},\ F \to \check{F}. \tag{6.3}$$

The first symmetry means that the $\partial\mathcal{E}_4$-Ellipsoid is centered around the origin. Any plane, passing through the origin, divides $\partial\mathcal{E}_4$ into the upper $\partial\mathcal{E}_4^{(+)}$, and the lower $\partial\mathcal{E}_4^{(-)}$ parts which, both, project onto the same sets. This may be seen clearly on the models in two, and three dimensions, cf. Fig. 2.

The second symmetry reduces the algebra involved by half, since the half of quantities of interest follow from previously found, by the v-operation.

7. The Projections of the 4-Ellipsoid Onto The (x,x'), (y,y'), and The (x,y)-Planes

To project the $\partial\mathcal{E}_4$ onto, let say, (x',y,y')-space, means to find a domain on which the coordinate x_+ of the upper branch $\partial\mathcal{E}_4^{(+)}$ (or, equivalently, the lower branch $\partial\mathcal{E}_4^{(-)}$), is defined. There are four distinct projections onto different three-dimensional spaces since the 4-Ellipsoid's equation can be solved for the $x_\pm$, $x'_\pm$ or the $y_\pm$ and $y'_\pm$ coordinates, cf. Fig. 2. In order to see this we write the 4-Ellipsoid's equation (6.1) in the four distinct forms:

$$ax^2+bx+c=0, \tag{7.1}$$

$$\check{a}y^2+\check{b}y+\check{c}=\left(ax^2+bx+c\right)^{\mathrm{v}}=0, \tag{7.2}$$

$$px'^2+qx'+r=0, \tag{7.3}$$

$$\check{p}y'^2+\check{q}y'+\check{r}=\left(px'^2+qx'+r\right)^{\mathrm{v}}=0, \tag{7.4}$$

where the coefficients are

$$a=F_{xx}, \tag{7.5}$$

$$b=2F_{xx'}x'+2F_{xy}y+2F_{xy'}y', \tag{7.6}$$

$$c=F_{x'x'}x'^2+2F_{x'y}x'y+2F_{x'y'}x'y'+F_{yy}y^2+2F_{yy'}yy'+F_{y'y'}y'^2-\lambda, \tag{7.7}$$

and

$$p=F_{x'x'}, \tag{7.8}$$

$$q=2F_{x'x}x+2F_{x'y}y+2F_{x'y'}, \tag{7.9}$$

$$r=F_{xx}x^2+2F_{xy}xy+2F_{xy'}xy'+F_{yy}y^2+2F_{yy'}yy'+F_{y'y'}y'^2-\lambda. \tag{7.10}$$

Solving Eq. (7.1), we get for the upper and the lower branches

$$x_\pm=\frac{1}{2a}\left(-b\pm\sqrt{b^2-4ac}\right)=x_\pm\left(x',y,y'\right), \tag{7.11}$$

$$y_\pm=\left(x_\pm\right)^{\mathrm{v}}=y_\pm\left(y',x,x'\right), \tag{7.12}$$

$$x'_\pm=\frac{1}{2p}\left(-q\pm\sqrt{q^2-4pr}\right)=x'_\pm\left(x,y,y'\right), \tag{7.13}$$

$$y'_\pm=\left(x'_\pm\right)^{\mathrm{v}}=y'_\pm\left(x,x',y\right). \tag{7.14}$$

It is understood that the solutions are real, which means that the following inequalities hold

$$b^2-4ac\geq 0, \tag{7.15}$$

$$\check{b}^2-4\check{a}\check{c}\geq 0, \tag{7.16}$$

$$q^2-4pr\geq 0, \tag{7.17}$$

$$\check{q}^2-4\check{p}\check{r}\geq 0. \tag{7.18}$$

They define the domains, solid 3-ellipsoids, on which the solutions $x_{\pm}$, etc., live. Hence, we found the projections of the 4-Ellipsoid, $\partial\mathcal{E}_4$, onto four, solid 3-ellipsoids, $\mathcal{E}_3$, $\check{\mathcal{E}}_3$ and M_3, $\check{M}_3$,

$$\mathcal{E}_3\left(x',y,y'\right)=Proj\left\{\partial\mathcal{E}_4^{(\pm)}/\mathcal{E}_3\left(x',y,y'\right)\right\}=\left\{x',y,y';b^2-4ac\geq 0\right\}, \tag{7.19}$$

$$\check{\mathcal{E}}_3\left(y',x,x'\right)=Proj\left\{\partial\mathcal{E}_4^{(\pm)}/\check{\mathcal{E}}_3\left(y',x,x'\right)\right\}=\left\{y',x,x';\check{b}^2-4\check{a}\check{c}\geq 0\right\}, \tag{7.20}$$

$$M_3\left(x,y,y'\right)=Proj\left\{\partial\mathcal{E}_4^{(\pm)}/M_3\left(x,y,y'\right)\right\}=\left\{x,y,y';q^2-4pr\geq 0\right\}, \tag{7.21}$$

$$\check{M}_3\left(y,x,x'\right)=Proj\left\{\partial\mathcal{E}_4^{(\pm)}/\check{M}_3\left(y,x,x'\right)\right\}=\left\{y,x,x';\check{q}^2-4\check{p}\check{r}\geq 0\right\}. \tag{7.22}$$

The surfaces, $\partial\mathcal{E}_3$ and ∂M_3, of these solid 3-ellipsoids correspond to loci of points on the 4-Ellipsoid, $\partial\mathcal{E}_4$, where the solutions x_+ and x_-, etc., coincide. They determine the boundaries of the projections, cf. Fig. 2. The loci are thus characterized by the conditions

$$\left\{x_+=x_-\right\}=\left\{b^2-4ac=0\right\}\xrightarrow{P}\partial\mathcal{E}_3\left(x',y,y'\right), \tag{7.23}$$

$$\left\{y_+=y_-\right\}=\left\{\check{b}^2-4\check{a}\check{c}=0\right\}\xrightarrow{P}\partial\check{\mathcal{E}}_3\left(y',x,x'\right), \tag{7.24}$$

$$\left\{x'_+=x'_-\right\}=\left\{q^2-4pr=0\right\}\xrightarrow{P}\partial M_3\left(x,y,y'\right), \tag{7.25}$$

$$\left\{y'_+=y'_-\right\}=\left\{\check{q}^2-4\check{p}\check{r}=0\right\}\xrightarrow{P}\partial\check{M}_3\left(y,x,x'\right). \tag{7.26}$$

In the second step, we project these 3-ellipsoids onto the (x,x'), (y,y') and the (x,y)-planes. That is we use only four, out of the twelve distinct possibilities to project the 3-ellipsoids onto the various coordinate planes, cf. Fig. 3. In principle, to find projections of these 3-ellipsoids, one could repeat the above construction, however, another way of projecting seems more appropriate in these imaginable cases.

In order to project, for example, the surface $\partial\mathcal{E}_3\left(x',y,y'\right)$ onto the (y,y')-plane, we slice it first with the planes

$$x'=c, \tag{7.27}$$

where the parameter c varies as it is indicated in Fig. 4, and project the intersecting ellipses onto the (y,y')-plane. Taking the envelope of the projected ellipses $\partial\mathcal{E}_2(c,y,y')$, with the respect to the parameter c, one gets the ellipse $-\partial\mathcal{E}_2(y,y')$. The final ellipse, which is composed of the $\partial\mathcal{E}_2(y,y')$, and its internal points, is now called the projection of the $\partial\mathcal{E}_4$ ellipsoid onto the (y,y')-plane

$$Proj\left\{\partial\mathcal{E}_4/(y,y')\right\} = \left[\mathcal{E}nv\partial\mathcal{E}_2(c,y,y')\right] = \mathcal{E}_2(y,y'). \tag{7.28}$$

The inclusion of the internal points is indicated by the solid brackets $[\ldots]$.

By projecting the slices, $y' = c$, onto the (x,x')-plane, and by taking their envelope, one finds the projection of the $\partial\mathcal{E}_4$ ellipsoid onto the (x,x')-plane

$$Proj\left\{\partial\mathcal{E}_4/(x,x')\right\} = \left[\mathcal{E}nv\partial\check{\mathcal{E}}_2(c,x,x')\right] = \check{\mathcal{E}}_2(x,x'). \tag{7.29}$$

Similarly, the slicing the $\partial M_3(x,y,y')$ with the planes $y' = c$, and the $\partial\check{M}_3(y,x,x')$ with the planes $x' = c$, and by finding the corresponding envelopes, one constructs two projections of the $\partial\mathcal{E}_4$ ellipsoid onto the (x,y)-plane,

$$Proj\left\{\partial\mathcal{E}_4/(x,y)\right\} = \left[\mathcal{E}nv\partial M_2(x,y,c)\right] = M_2(x,y), \tag{7.30}$$

and

$$Proj\left\{\partial\mathcal{E}_4/(x,y)\right\} = \left[\mathcal{E}nv\partial\check{M}_2(y,x,c)\right] = \check{M}_2(y,x). \tag{7.31}$$

It is not clear, at this point, that both projections M_2 and $\check{M}_2$ of the 4-Ellipsoid, onto the (x,y)-plane, coincide. This is because our method of projecting consists of two steps. In the second step one considers projection of a projection, resulting from the first step. Since the two different intermediate projections are involved, it is not obvious that they will yield the same final projection.

To find the envelopes one has to eliminate the parameters x', y' from the supplementary conditions

$$a.\quad \frac{\partial}{\partial x'}\left(b^2 - 4ac\right) = 0, \tag{7.32}$$

$$b.\quad \frac{\partial}{\partial y'}\left(\check{b}^2 - 4\check{a}\check{c}\right) = 0, \tag{7.33}$$

$$c.\quad \frac{\partial}{\partial y'}\left(q^2 - 4pr\right) = 0, \tag{7.34}$$

$$d.\quad \frac{\partial}{\partial x'}\left(\check{q}^2 - 4\check{p}\check{r}\right) = 0. \tag{7.35}$$

The first two conditions yield

$$x' = Ay + By', \tag{7.36}$$

$$y' = \check{A}x + \check{B}x'. \tag{7.37}$$

Similarly, for the conditions *c.* and *d.* one finds the solutions

$$y' = Px + Qy, \tag{7.38}$$

$$x' = \check{P}y + \check{Q}x. \tag{7.39}$$

where the coefficients are

$$A = \Delta^{-1}\left(F_{xx'}F_{xy} - F_{xx}F_{x'y}\right), \tag{7.40}$$

$$B = \Delta^{-1}\left(F_{xx'}F_{xy'} - F_{xx}F_{x'y'}\right), \tag{7.41}$$

$$P = \nabla^{-1}\left(F_{x'y'}F_{xx'} - F_{x'x'}F_{xy'}\right), \tag{7.42}$$

$$Q = \nabla^{-1}\left(F_{x'y'}F_{x'y} - F_{x'x'}F_{yy'}\right), \tag{7.43}$$

and for the denominators Δ and ∇ we get

$$\Delta = F_{xx}F_{x'x'} - F_{xx'}^2 > 0, \tag{7.44}$$

$$\nabla = F_{x'x'}F_{y'y'} - F_{x'y'}^2 > 0. \tag{7.45}$$

Substituting the solutions (7.36) - (7.39), back into the conditions (7.23) - (7.26), we obtain the equations of the ellipses $\partial\mathcal{E}_2(y, y')$, $\partial\check{\mathcal{E}}_2(x, x')$, and $\partial M_2(x, y)$, $\partial\check{M}_2(y, x)$,

$$\partial\mathcal{E}_2: \quad \mathcal{E}_{yy}y^2 + 2\mathcal{E}_{yy'}yy' + \mathcal{E}_{y'y'}y'^2 = \lambda, \tag{7.46}$$

$$\partial\check{\mathcal{E}}_2: \quad \check{\mathcal{E}}_{yy}x^2 + 2\check{\mathcal{E}}_{yy'}xx' + \check{\mathcal{E}}_{y'y'}x'^2 = \lambda, \tag{7.47}$$

$$\partial M_2: \quad M_{xx}x^2 + 2M_{xy}xy + M_{yy}y^2 = \lambda, \tag{7.48}$$

$$\partial\check{M}_2: \quad \check{M}_{xx}y^2 + 2\check{M}_{xy}xy + \check{M}_{yy}x^2 = \lambda, \tag{7.49}$$

where the coefficients are given in terms of the F's. Up to the second order in the q's the coefficients are

$$\mathcal{E}_{yy} = F_{yy} + (\sin\mu_x)^{-1}\left(F_{xy}^2 + F_{x'y}^2\right) + \ldots, \tag{7.50}$$

$$\mathcal{E}_{yy'} = F_{yy'} + (\sin\mu_x)^{-1}\left(F_{xy}F_{xy'} + F_{x'y'}F_{x'y}\right) + \ldots, \tag{7.51}$$

$$\mathcal{E}_{y'y'} = F_{y'y'} + (\sin \mu_x)^{-1} \left(F_{xy'}^2 + F_{x'y'}^2 \right) + \ldots, \tag{7.52}$$

$$M_{xx} = F_{xx} + (\sin \mu_y)^{-1} F_{xy'}^2 + \ldots = \check{M}_{yy}, \tag{7.53}$$

$$M_{xy} = F_{xy} + \ldots = \check{M}_{xy}, \tag{7.54}$$

$$M_{yy} = F_{yy} + (\sin \mu_x)^{-1} F_{x'y}^2 + \ldots = \check{M}_{xx}. \tag{7.55}$$

Thus we have arrived at our goal; the solid ellipses $\mathcal{E}_2$, $\check{\mathcal{E}}_2$, M_2, $\check{M}_2$ constitute the projections of the invariant 4-Ellipsoid onto the (y, y'), (x, x') and the (x, y)-planes. Notice, that up to the second order in the q's, the equations (7.48) and (7.49) coincide. Thus we obtain the same projection of the invariant 4-Ellipsoid onto the (x, y)-plane, independent of the intermediate steps involved.

8. Possible Measures of the Thick Ellipse Effect

Let us denote (the projected emittance, in absence of the linear coupling),

$$\begin{aligned} \epsilon_x &= \lambda \left(-\sin \mu_x\right)^{-1}, \\ \epsilon_y &= \lambda \left(-\sin \mu_y\right)^{-1}, \end{aligned} \tag{8.1}$$

and let us rewrite Eqs. (7.46) - (7.49), for the projections, as follows

$$a. \quad e_{yy} y^2 + e_{yy'} 2yy' + e_{y'y'} y'^2 = \epsilon_y, \tag{8.2}$$

$$b. \quad \check{e}_{yy} x^2 + \check{e}_{yy'} 2xx' + \check{e}_{y'y'} x'^2 = \epsilon_x, \tag{8.3}$$

$$c. \quad m_{xx} \epsilon_x^{-1} x^2 + m_{xy} \left(\epsilon_x \epsilon_y\right)^{-1/2} 2xy + m_{yy} \epsilon_y^{-1} y^2 = 1, \tag{8.4}$$

$$d. \quad \check{m}_{xx} \epsilon_y^{-1} y^2 + \check{m}_{xy} \left(\epsilon_x \epsilon_y\right)^{-1/2} 2xy + \check{m}_{yy} \epsilon_x^{-1} x^2 = 1, \tag{8.5}$$

(equivalent to the previous equation), where the new coefficients are

$$e_{yy} = \left(-\sin \mu_y\right)^{-1} \mathcal{E}_{yy}, \tag{8.6}$$

$$e_{yy'} = \left(-\sin \mu_y\right)^{-1} \mathcal{E}_{yy'}, \tag{8.7}$$

$$e_{y'y'} = \left(-\sin \mu_y\right)^{-1} \mathcal{E}_{y'y'}, \tag{8.8}$$

and

$$m_{xx} = \left(-\sin \mu_x\right)^{-1} M_{xx}, \tag{8.9}$$

$$m_{xy} = \left(\sin \mu_x \sin \mu_y\right)^{-1/2} M_{xy}, \tag{8.10}$$

$$m_{yy} = \left(-\sin \mu_y\right)^{-1} M_{yy}. \tag{8.11}$$

Putting the skew-quadrupole strengths, q's, equal to zero, one gets from the formula (7.50) - (7.55), and from the formula (5.3) - (5.12), the results

$$\begin{aligned} e_{yy}\Big|_0 = 1, \quad e_{yy'}\Big|_0 = 0, \quad e_{y'y'}\Big|_0 = 1, \\ m_{xx}\Big|_0 = 1, \quad m_{xy}\Big|_0 = 0, \quad m_{yy}\Big|_0 = 1. \end{aligned} \tag{8.12}$$

Hence, we recover the familiar invariant Courant-Snyder circles, in the (x, x'), and (y, y')-planes

$$y^2 + y'^2 = \epsilon_y, \tag{8.13}$$

and

$$x^2 + x'^2 = \epsilon_x, \tag{8.14}$$

and the ellipse in the (x, y)-plane

$$\frac{x^2}{\epsilon_x} + \frac{y^2}{\epsilon_y} = 1. \tag{8.15}$$

Both ellipses, (8.4) and (8.5), coincide in the zero-coupling limit, cf. Fig. 5. Areas in between the curves with, and without the coupling, are available for the spread of a trajectory when the linear coupling is present. For this reason we propose to consider the characteristic dimensions, δ's, of these areas as a measure of the Thick Ellipse Effect. They are related to the coefficients e's and m's as follows, (in the same order as shown in Fig. 5),

$$a. \quad \delta_y = \left[(e_{yy})^{-1/2} - 1\right]\sqrt{\epsilon_y}, \quad \delta_{y'} = \left[(e_{y'y'})^{-1/2} - 1\right]\sqrt{\epsilon_y}, \tag{8.16}$$

$$b. \quad \delta_x = \left[(\check{e}_{yy})^{-1/2} - 1\right]\sqrt{\epsilon_x}, \quad \delta_{x'} = \left[(\check{e}_{y'y'})^{-1/2} - 1\right]\sqrt{\epsilon_x}, \tag{8.17}$$

$$c. \quad \delta_x = \left[(m_{xx})^{-1/2} - 1\right]\sqrt{\epsilon_x}, \quad \delta_y = \left[(m_{yy})^{-1/2} - 1\right]\sqrt{\epsilon_y}, \tag{8.18}$$

or, equivalently, the last thicknesses can be expressed as

$$d. \quad \delta_x = \left[(\check{m}_{yy})^{-1/2} - 1\right]\sqrt{\epsilon_x}, \quad \delta_y = \left[(\check{m}_{xx})^{-1/2} - 1\right]\sqrt{\epsilon_y}. \tag{8.19}$$

The areas in between the curves can be expressed via the above thicknesses, δ's, and via the mixed coefficients $e_{yy'}$ and m_{xy}. For example, for the case a. we have the result

$$\delta A = \left[\left(e_{yy}e_{y'y'} - e_{yy'}^2\right)^{-1/2} - 1\right]\pi\epsilon_y, \tag{8.20}$$

and similar for the other cases. We will return to this point after averaging over the random q's, which will simplify the considerations.

9. Averaging Over the Random Skew-Quadrupole Strengths. RHIC - An Example

Assuming that the q's are normally distributed random variables, we have

$$< q_r > = 0, \tag{9.1}$$

and

$$< q_r^2 > = G_0^2/N, \quad r = 1, \ldots, N. \tag{9.2}$$

Further, assuming that, for both x and y directions

$$< \sin \mu^r > =< \cos \mu^r >= 0, \tag{9.3}$$

and

$$< \sin^2 \mu^2 > =< \cos^2 \mu^r >= 1/2, \tag{9.4}$$

while the averages of mixed products assumed to vanish, we get for the averages of the driving terms

$$< d^{(1)} > = 0, \tag{9.5}$$

$$< d^{(2)} > = 0, \tag{9.6}$$

$$< d^{(1)^2} > = 1/4G_0^2. \tag{9.7}$$

The averages of squares of the second-order driving terms are small. The averages of products of different first-order driving terms vanish.

For the averages of the coefficients e and m we get the results

$$< e_{yy'} > =< m_{xy} >= 0, \tag{9.8}$$

$$< e_{yy} > =< e_{y'y'} >= 1 - \kappa/4, \tag{9.9}$$

and

$$< m_{xx} > =< m_{yy} >= 1 - \kappa/8, \tag{9.10}$$

where the parameter κ is

$$\kappa = G_0^2 \left(\sin \mu_x \sin \mu_y\right)^{-1}. \tag{9.11}$$

For the averages of the conjugate coefficients one has, in general

$$< \check{e} >=< e >^{\mathrm{v}}, \quad < \check{m} >=< m >^{\mathrm{v}}. \tag{9.12}$$

The equations (8.2) and (8.3), after the averaging become

$$y^2 + y'^2 =< \tilde{\epsilon}_y >, \tag{9.13}$$

$$x^2 + x'^2 =< \tilde{\epsilon}_x >, \tag{9.14}$$

where, according to the formula (9.8), we have

$$< \tilde{\epsilon}_x > /\epsilon_y =< \tilde{\epsilon}_x > /\epsilon_x =< e_{yy} >^{-1}= 1 + \kappa/4. \tag{9.15}$$

The equations (8.4) and (8.5), both, yield the same equation

$$x^2/ < \tilde{\epsilon}_x >' + y^2/ < \tilde{\epsilon}_y >'= 1, \tag{9.16}$$

where the new average projected emittance is given by the relations

$$< \tilde{\epsilon}_x >' /\epsilon_x =< \tilde{\epsilon}_y >' /\epsilon_y = 1 + \kappa/8. \tag{9.17}$$

Corresponding to the equations (9.13), (9.14) average characteristic dimensions are

$$< \delta_y >_a =< \delta_{y'} >_a= \kappa/8\sqrt{\epsilon_y}, \tag{9.18}$$

and

$$< \delta_x >_b =< \delta_{x'} >_b= \kappa/8\sqrt{\epsilon_x}. \tag{9.19}$$

The average characteristic thicknesses corresponding to Eq. (9.16) are even smaller

$$< \delta_x >_c = \kappa/16\sqrt{\epsilon_x}, \tag{9.20}$$

and

$$< \delta_y >_c = \kappa/16\sqrt{\epsilon_y}. \tag{9.21}$$

The average areas in between the curves in Figs. 5a and b, are according to formula (8.20), equal to

$$< \delta A >_a = \kappa/4\pi\epsilon_y, \tag{9.22}$$

and

$$< \delta A >_b = \kappa/4\pi\epsilon_x. \tag{9.23}$$

For the case c., in Fig. 5, one gets the result

$$< \delta A >_c= \kappa/8\pi\sqrt{\epsilon_x\epsilon_y}. \tag{9.24}$$

Thus, all the relevant quantities are expressed through the parameter κ, which, for case of RHIC, where

$$\mu_x = 2\pi \times 28.827, \quad \sin\mu_x = -0.885,$$

and

$$\mu_y = 2\pi \times 28.823, \quad \sin\mu_y = -0.896, \tag{9.25}$$

and

$$G_0 = 0.25,$$

is equal to

$$\kappa = G_0^2 \left(\sin\mu_x \sin\mu_y\right)^{-1} = 0.007, \quad \text{(RHIC)}.$$

Therefore, we obtain the following numerical characteristics of the Thick Ellipse Effect, produced by the random skew-quadrupoles, in RHIC

$$\begin{aligned}
&< e_{yy} > =< e_{y'y'} >=< m_{xx} >=< m_{yy} >= 0.99,\\
&< \tilde{\epsilon}_y > /\epsilon_y =< \tilde{\epsilon}_x > /\epsilon_x = 1.017,\\
&< \tilde{\epsilon}_y >' /\epsilon_y =< \tilde{\epsilon}_x >' /\epsilon_x = 1.008,\\
&< \delta_y >_a =< \delta_{y'} >_a = 0.008\ \sqrt{\epsilon_y},\\
&< \delta_x >_b =< \delta_{x'} >_b = 0.008\ \sqrt{\epsilon_x},\\
&< \delta_x >_c = 0.004\ \sqrt{\epsilon_x},\\
&< \delta_y >_c = 0.004\ \sqrt{\epsilon_y},\\
&< \delta A >_a = 0.017\ \pi\epsilon_y,\\
&< \delta A >_b = 0.017\ \pi\epsilon_x,\\
&< \delta A >_c = 0.008\ \pi\sqrt{\epsilon_x\epsilon_y}.
\end{aligned} \tag{9.26}$$

10. Influence of the Tune Splitting Correction on the Thick Ellipse Effect

An assumption that the new tunes, μ_1 and μ_2, coincide lies at the heart of our choice of the linear in T invariant. In other words it is tacitly assumed that the tune splitting produced by the linear coupling has been corrected. One knows[3,4,5] that this implies vanishing of all the first order, and some of the second-order driving terms

$$d^{(1)}_{...} = 0, \tag{10.1}$$

and

$$d^{(2)}_{cc} + d^{(2)}_{ss} = 0, \tag{10.2}$$

$$\check{d}^{(2)}_{cc} + \check{d}^{(2)}_{ss} = 0. \tag{10.3}$$

As the result, the averaged coefficients e, m become negligible small (at the point $s = 0$, where the tune splitting correction is done).

One has, in particular,

$$< e_{...} > \Big|_{\Delta\nu=0} = e_{...}\Big|_{q=0}, \tag{10.4}$$

$$< m_{...} > \Big|_{\Delta\nu=0} = m_{...}\Big|_{q=0}, \tag{10.5}$$

and, as the result the Thick Ellipse Effect vanishes, at the point of the tune splitting correction

$$< \delta > \Big|_{\Delta\nu=0} = \delta\Big|_{q=0} = 0, \tag{10.6}$$

and

$$< \delta A > \Big|_{\Delta\nu=0} = \delta A\Big|_{q=0} = 0. \tag{10.7}$$

11. Matching Conditions at the Observation Point

The averaged equations (9.13), and (9.14) suggest, that one can match the linearly coupled beam, at the point of observation, $s = 0$, by a beam with modified machine parameters. Writing these equations as (machine ellipse equations, in the original phase-space coordinates)

$$\tilde{X}\rho_x^{-1}X = \tilde{\epsilon}_x, \tag{11.1}$$

and

$$\tilde{Y}\rho_y^{-1}Y = \tilde{\epsilon}_y, \tag{11.2}$$

where

$$\rho_x = \begin{pmatrix} \tilde{\beta}_x & -\tilde{\alpha}_x \\ -\tilde{\alpha}_x & \tilde{\gamma}_x \end{pmatrix}, \tag{11.3}$$

and similar for ρ_y, we find the following matching conditions, at the point of observation,

$$\tilde{\alpha}_x = \alpha_x = 0, \tag{11.4}$$

$$\tilde{\beta}_x = \beta_x, \tag{11.5}$$

and

$$\tilde{\epsilon}_x = < \tilde{\epsilon}_x > = (1 + \kappa/4)\,\epsilon_x, \tag{11.6}$$

and similar for the y- parameters.

12. Concluding Remarks

A method of constructing projections of the invariant 4-Ellipsoid onto various planes of interest, is described. It can be applied to any invariant surfaces in the four-dimensional phase-space, including those corresponding to the non-linear coupling, as well.

Contribution of skew-quadrupole errors to the Thick Ellipse Effect, in RHIC, was found small. Hence, by large, the non-linear effects are responsible for the smears of the invariant curves, observed in the computer simulations in RHIC. Their treatment, however, requires employment of rather different methods, than those used here, which are suitable for the linear coupling case. We calculate an impact of the linear coupling, up to the second order in the skew-quadrupole strengths, on various quantities of interest. It seems, that our averaged projected equations, (9.13) and (9.14), can be useful when matching linearly coupled beams at the injection point in RHIC - for example.

The invariant equations (7.46) and (7.47) or, equivalently, the equations (8.2) and (8.3) provide a counterpart of the familiar Courant-Snyder invariants when the linear coupling is present. Notice, that they are written in the normalized coordinates.

13. Acknowledgments

The problem of the Thick Ellipse Effect, due to the linear coupling, was suggested by Harald Hahn. Vivid discussions with Sandro Ruggiero, concerning the four dimensional phase-space, were helpful in conceiving the idea of projection from four to two dimensions. Acknowledgments go also to Fritz Dell for providing his results on the computer simulations of the Thick Ellipse Effect, in RHIC, and for reading the manuscript.

14. References

1. E.D. Courant and H.S. Snyder, Ann. Phys. 3, 1 (1958).
2. D.A. Edwards and L.C. Teng, IEEE Trans. Nucl. Sci., Vol. NS-20, No. 3, p. 885 (1973), see also

   L.C. Teng, "Concerning N-Dimensional Coupled Motions," Fermilab Report FN-229 (1971), and "Coupled Transverse Motion", FNAL-TM-1566 (1989).
3. A.G. Ruggiero, "The Problem of Linear Coupling - Parts I, II and III," Talks at Accelerator Physics Division Meetings, May 16, 23 and 30 (1991), BNL, see also

   A.G. Ruggiero, "Exact Analysis to any Order of the Linear Coupling Problem in the Thin Lens Model," 5th ICFA Advanced Beam Dynamics Workshop, Corpus Christi, Texas, October 3-8, 1991.
4. V. Garczynski, "Beta-Function Distortions Due to Linear Coupling," BNL AD/AP Technical Note No. 24, (August 1991).
5. V. Garczynski, "The Tune Shift Due to Linear Coupling," BNL AD/AP Technical Note No. 25, (August 1991).
6. V. Garczynski, "Emittance Change Due to Linear Coupling - Possible Correction Scheme of Emittance Growth," BNL AD/AP Technical Note No. 28, (September 1991).

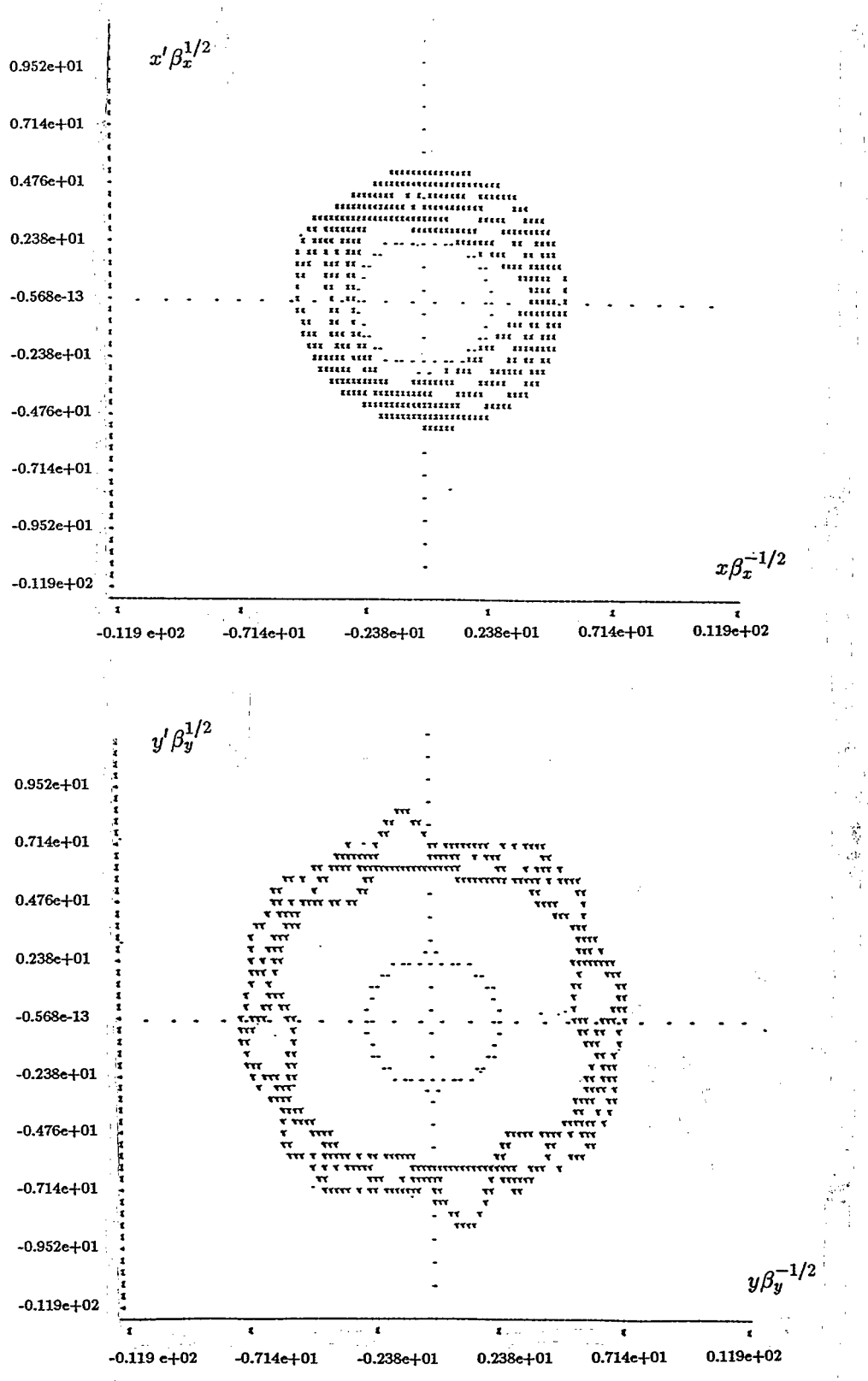

Figure 1: The Thick Ellipse Effect in computer simulations of the x-y coupling in RHIC (courtesy of G. Fritz Dell).

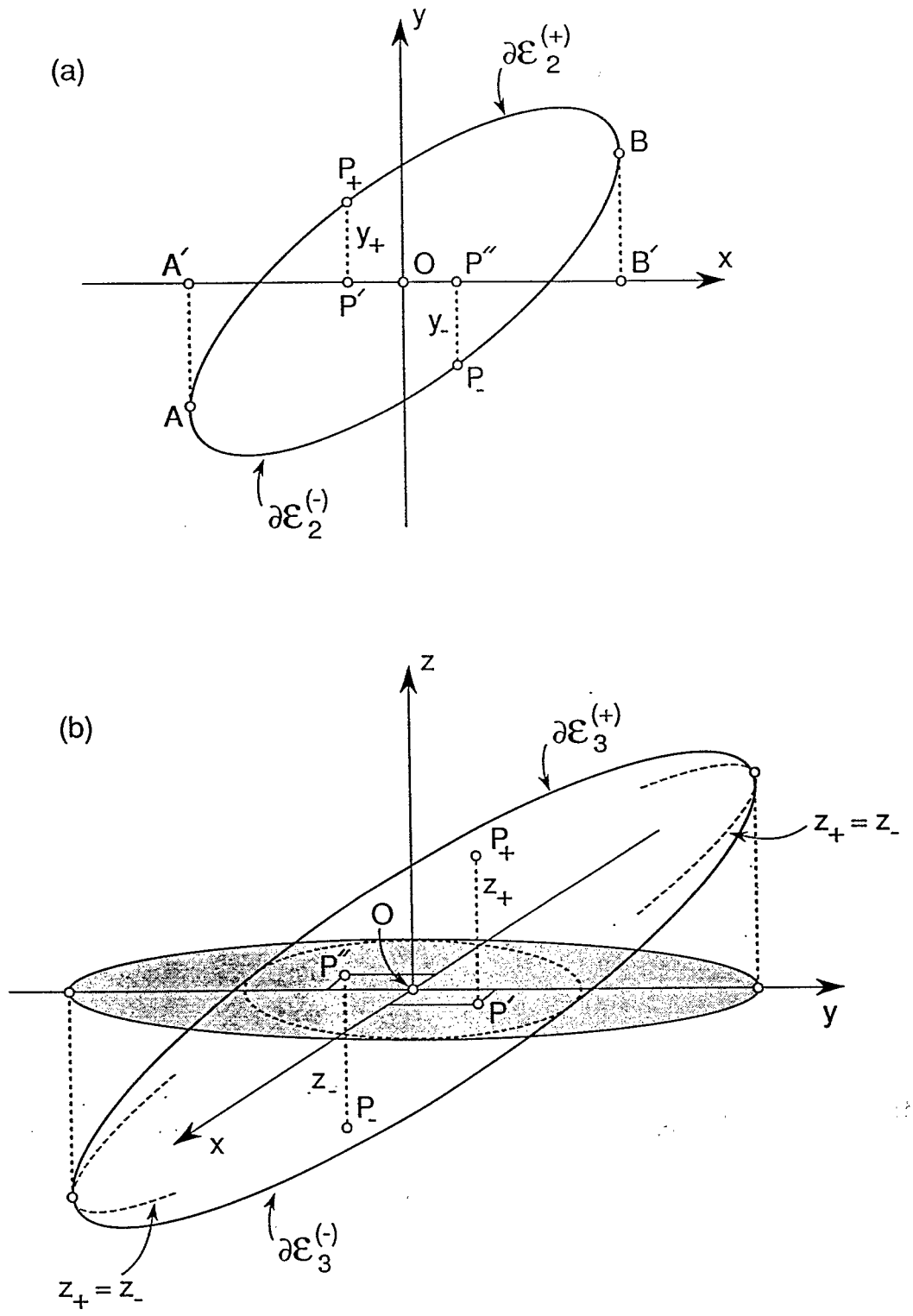

Figure 2: Projections of the upper y_+ (z_+), and the lower y_- (z_-) branches of the ellipse, a. (ellipsoid, b.) coincide, and are symmetrically centered around the origin 0.

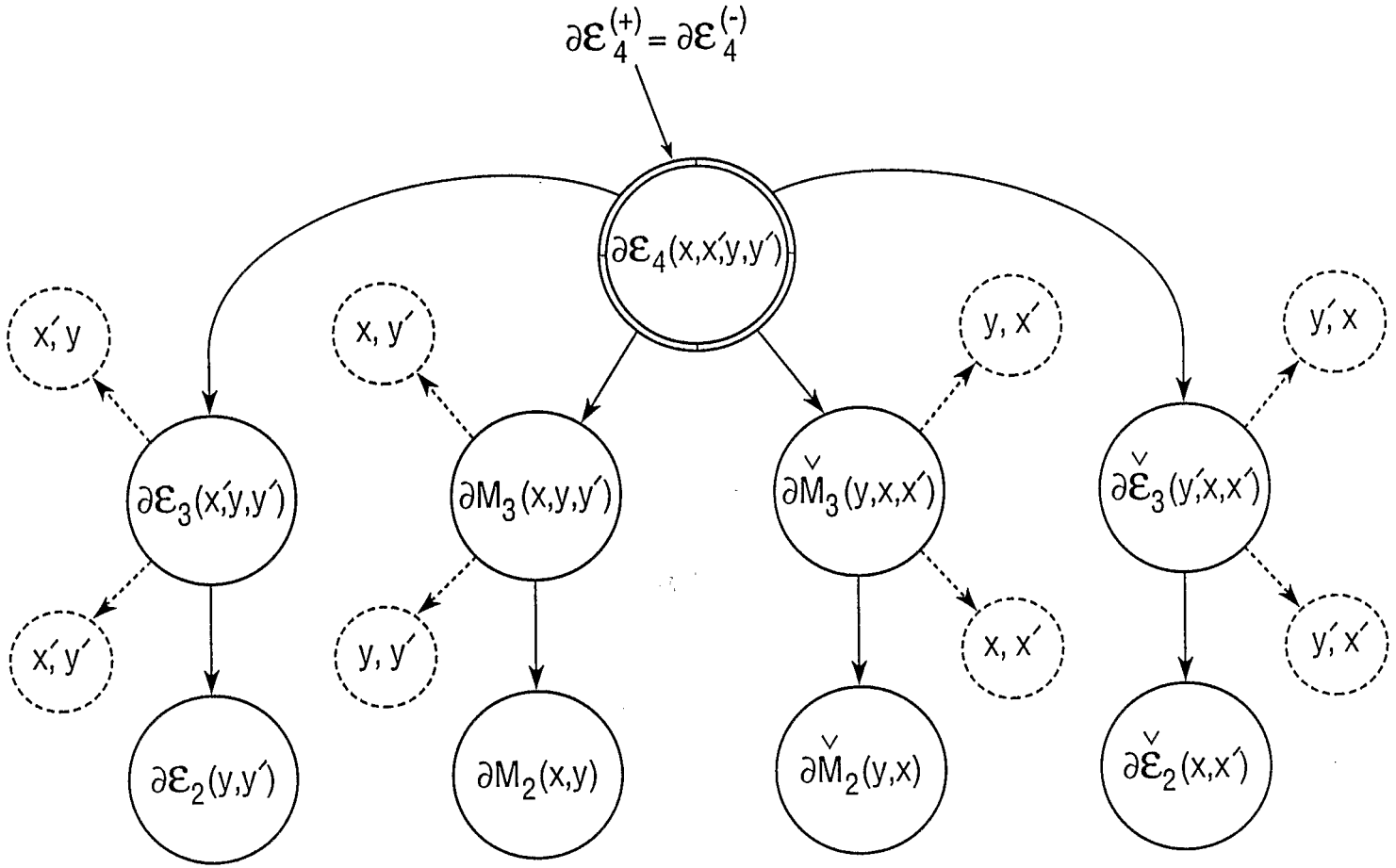

Figure 3: Projections of the $\partial\mathcal{E}_4$ onto the three-dimensional ellipsoids, and the ellipses of interest, as indicated by the arrows. Eight, unused possibilities are indicated by the broken arrows, and circles.

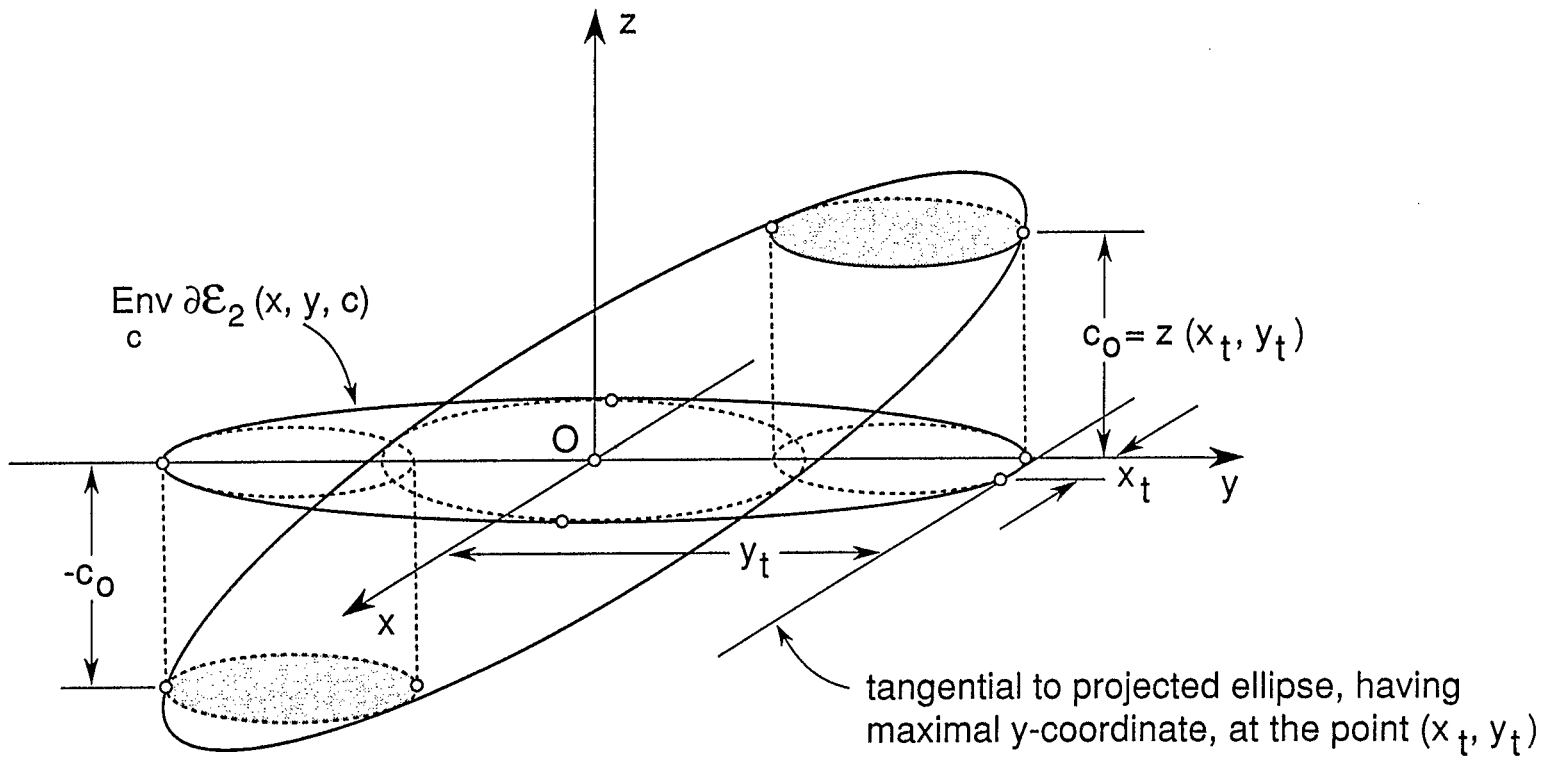

Figure 4: Slicing of the 3-ellipsoid with the planes; $z = c$, $-c_0 \leq c \leq c_0$ and projecting the intersecting ellipses onto the (x, y)-plane. The projected ellipses posses the (elliptic) envelope.

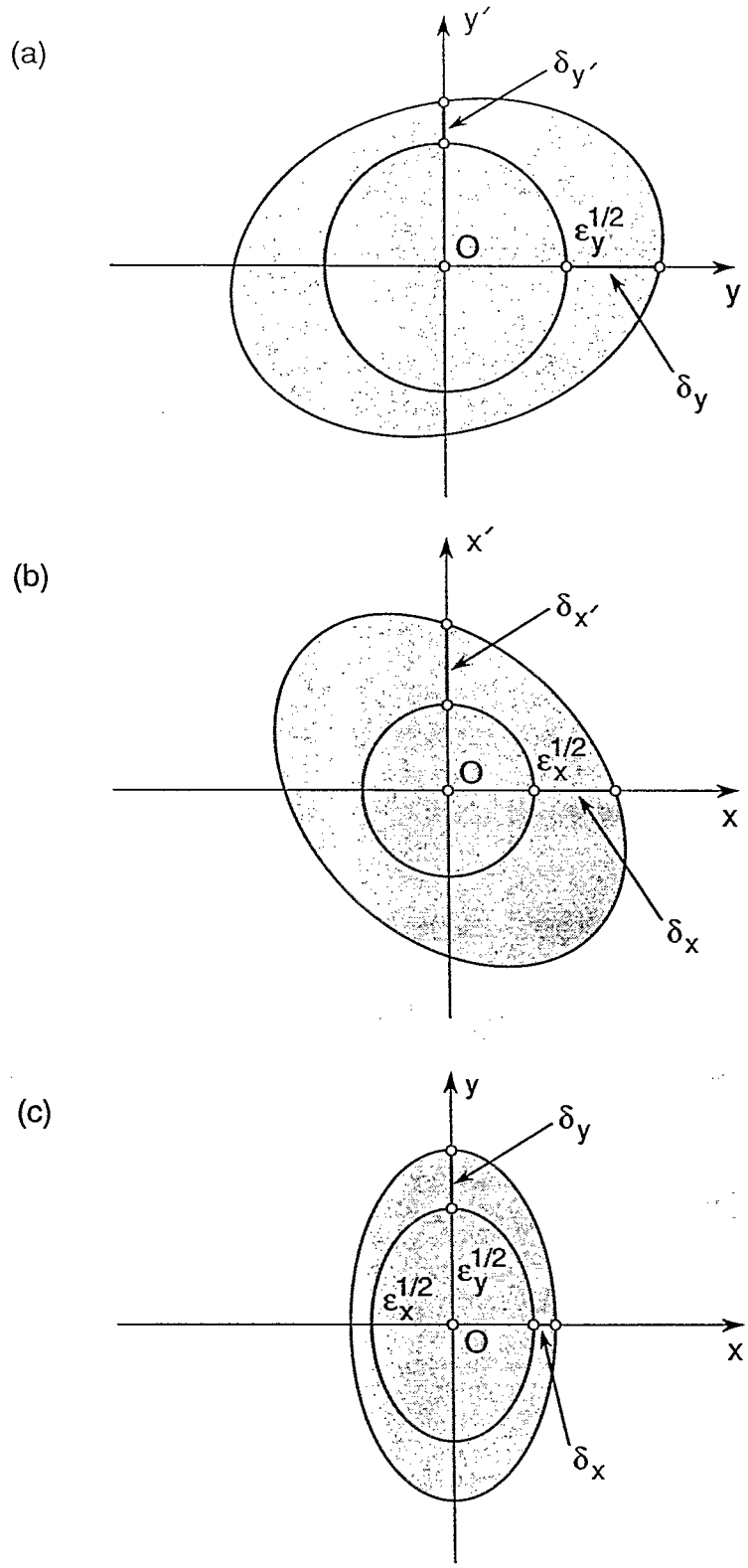

Figure 5: The Thick Ellipse Effect produced by the linear coupling. The outer ellipses correspond to Eqs. (8.2) - (8.4), while the inner curves correspond to Eqs. (8.13) - (8.15).